ANNALES
UNIVERSITATIS MARIAE CURIE-SKŁODOWSKA
LUBLIN – POLONIA
VOL. LXX SECTIO AAA 2015

DYNAMIC EFFECTS AND LARGE – AMPLITUDE MOTION IN JACOBI AND POINCARÉ SHAPE TRANSITIONS IN ATOMIC NUCLEI

K. Mazurek[1], J. Dudek[2], A. Maj[1], M. Kmiecik[1] and D. Rouvel[2]

[1]The Niewodniczański Institute of Nuclear Physics, Polish Academy of Sciences
ul. Radzikowskiego 152, Pl-31-342 Kraków, Poland
[2]IPHC/DRS and Université de Strasbourg, 23 rue du Loess
B.P. 28, F-67037 Strasbourg Cedex 2, France

ABSTRACT

The Jacobi and Poincaré shape transitions are very promising way to investigate the shape of the nucleus. The presented here quasi-phenomenological approach allows to estimate the experimental conditions which are necessary to observe these phenomena. The static energy minimum gives the spin ranges and the fissility of atomic nuclei soft for the shape transitions and available experimentally. Dynamical effects taken into account through the solving collective Hamiltonian for zero-point vibration estimation, changes the spin rages for the shape transitions. The static deformation of the nucleus constrained by the minimum of energy for given spin has been enhanced to dynamical nuclear shapes permitted by the zero point energy. The large amplitude vibrations around the static deformation gives the ensemble of nuclear shapes possible to be observed.

Keywords: shape transition, collective Hamiltonian, zero-point vibration, rotating nucleus

1. INTRODUCTION

The symmetries and the shape transition problem fascinated humanity since early times of the history. In particular, Colin Maclaurin, a mathematician of the seventeen century showed that with increasing velocity of rotation, an originally spheroid begins flattening with resulting oblate shapes. These theoretical studies were followed by Carl Gustav Jacob Jacobi. He provided the mathematical arguments, according to which a flat rotating object such as the Earth, could change its shapes with increasing velocity of rotation and deform towards the elongated, prolate shapes at the fast enough rotation [1]. The critical values of rotation velocity at which objects change its shapes has been called 'bifurcation point'. Following this discussion, a French mathematician and astronomer Jules Henri Poincaré suggested another possibility for the shape changes, namely, from the left-right symmetric prolate to the left-right asymmetric pear-like shapes [2]. These phenomena predicted originally for astronomical objects were predicted to exist in micro-scale physics – in nuclei [3].

The calculations whose results are presented below address exotic shape transitions of fast rotating nuclei. The total energy of the nucleus depends on its shape. The ground state deformation is estimated usually by finding the set of deformation parameters, which gives the lowest possible energy. The energy in the ground state defines the mass of the nucleus. There exist various methods of calculating the nuclear masses with precision varying slightly from one approach to another, e.g. Hartree-Fock-Bogoluybov method, macroscopic-microscopic method [4, 5, 6] or the Energy Density Functional methods [7, 8, 9]. Each of this approaches could predict various properties of the static nuclei but the description of the highly excited systems is usually more challenging.

In this article the main focus will be to address the behavior of hot nuclei. At sufficiently high temperatures one can use the macroscopic nuclear models since the shell effects are known to vanish with increasing temperature. We will use one of the recent macroscopic nuclear model realizations in the form of the Lublin-Strasbourg Drop (LSD) [10, 11]. In this approach the parameters are adjusted to the nuclear masses whereas at the same time the fission barriers of the heavy nuclei are well reproduced. The implementation of this approach within the Thermal Shape Fluctuation Model well describes the shape of the effective strength function of the Giant Dipole Resonances (GDR) in hot rotating compound nuclei. Therefore it allows to suggest that the same approach will be suitable to study the shape transitions other than the Jacobi shape transition [12].

The intrinsic components of the macroscopic energy of the rotating nucleus are the energy terms associated with the volume-, surface-, Coulomb-, curvature- and rotation contributions which are derived from the geometrical properties of the nucleus. An additional concept which helps to reproduce the fission barriers in the medium-mass nuclei is the one of the congruence energy; although its microscopic origin is not well under control, the associated term gives the strongest extra binding energy for the nuclei in which the numbers of neutrons and protons are equal [13].

The Jacobi shape transitions, which are manifested by changing the deformation of the object from oblate, through triaxial to prolate when spin increases, has been investigated theoretically [15] and experimentally [14, 16, 12, 17, 18, 19]. However, the Poincaré transitions from a left-right symmetric – to asymmetric objects are challenging experimentally; so far a few theoretical estimates can be found e.g. in [20, 21, 22].

2. POTENTIAL ENERGY SURFACES

As it is well known, the nuclear energy depends generally on the geometrical shape. The experimental observables, which can help to constraint the potential energy of the nucleus are the mass and the fission barrier heights; one can also indirectly use the information about the fission fragment distributions and the total kinetic energy spectra.

One of the standard, convenient parametrizations of the nuclear surface is based on using the spherical harmonic $Y_{\lambda,\mu}$ basis:

$$\mathcal{R}(\theta,\phi) = R_0 c(\{\alpha_{\lambda,\mu}\})\left(1 + \sum_{\lambda=2}^{\lambda_{max}} \sum_{\mu=-\lambda}^{\lambda} \alpha_{\lambda,\mu} Y_{\lambda,\mu}(\theta,\phi)\right). \tag{1}$$

where function $c(\{\alpha_{\lambda,\mu}\})$ assures the volume conservation condition. The deformations $\alpha_{\lambda,\mu=0} \neq 0$ lead to axially symmetric shapes. The pear-shape deformations are obtained with $\alpha_{\lambda=3,\mu=0} \neq 0$. As the center of coordinate space is not always equivalent to the center of nuclear mass, the Huygens–Steiner theorem is applied for rotation.

In this article we use a phenomenological parameterization of the so-called congruence energy term [cf. [23] and references therein]:

$$E_{cong}(\alpha_{20}) = W_0(Z,N) \cdot F_{neck}(\alpha_{20}), \tag{2}$$

where

$$F_{neck}(\alpha_{20}) = 1 + \tfrac{1}{2}\left\{1 + \tanh\left[(\alpha_{20} - \alpha_{20}^0)/a_{neck}\right]\right\}. \tag{3}$$

The Wigner energy term, W_0, is parametrized as in [24], i.e.:

$$W_0(Z,N) = -C_0 \exp(-W|I|/C_0) \quad \text{with} \quad I = (N-Z)/A. \tag{4}$$

where $C_0 = 10$ MeV and $W = 42$ MeV.

Figure 1 shows the difference of the fission barrier heights (left) and the energy minima (right) calculated with and without congruence energy term. The potential energy was minimized over axial even and odd λ parameters up to $\lambda = 12$. The lowest energy at any given spin defines the yrast line. The fission barier height is defined as the difference between the saddle point and energy in the potential minimum.

Calculations show that the non-axial deformation parameters are less important [23]. The fission barier heights obtained with congruence energy are always lower.

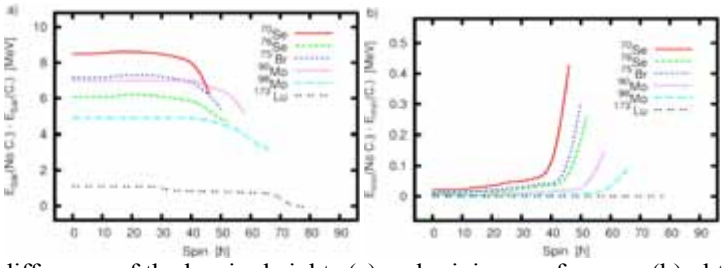

Figure 1: The difference of the barrier heights (a) and minimum of energy (b) obtained with and without congruence-energy term in function of the spin for ^{70,76}Se, ^{75}Br, ^{90,98}Mo, ^{173}Lu, ^{228}Ra and ^{252}Cf.

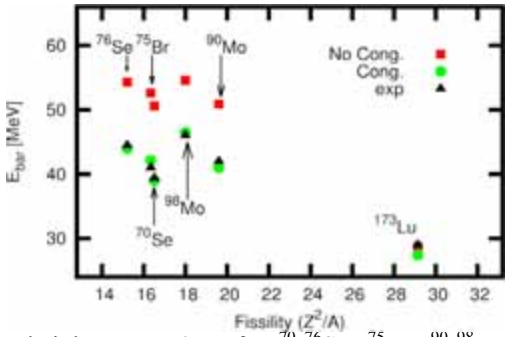

Figure 2: Fission barrier heights at L=0 $\hbar$ for ^{70,76}Se, ^{75}Br, ^{90,98}Mo, ^{173}Lu. The barrier heights for the calculation made with and without the congruence energy included compared to the experimental data (the error bars are shown but too small to be visible) [25, 26, 27, 28]

The full effect of the congruence term on physical observables such as the fission barriers is displayed in Fig. 2. There exist sufficiently many nuclei for which the experimental fission barriers are known in the actinide and heavy nuclei but in the medium mass nuclei only a few results can be found. As we are mostly interested here in the medium-mass nuclei, Fig. 2 shows the barrier height for only one heavy nucleus as a reference point. The barrier heights for heavy nuclei are almost not affected by adding the congruence term in the form proposed in Eq. (2).

More tests and discussion about the new form of congruence energy are available in Ref. [23].

3. JACOBI AND POINCARÉ TRANSITIONS

The procedure of finding nuclei and spin ranges in which the shape transitions take place begins with the calculation of the macroscopic energy in

a multidimensional deformation space, for each angular momentum separately. The calculation are done for a set of $\{\alpha_{\lambda,\mu}\}$ deformations, where $\lambda = 2,3,\ldots,12$ and $\mu = 0$, and, additionally, the quadrupole non axial parameter $\alpha_{2,2}$ is taken into account. This choice ensures that we consider a sufficiently rich set of axially deformed nuclear shapes. Looking for the Jacobi transitions, we have minimized the energy over deformation parameters $\lambda = 3,\ldots,12$ and projected the energy onto the 2D-space $(\alpha_{20},\alpha_{22})$, cf. Fig. 3.

The Poincaré shape transitions are manifested by symmetry-breaking in which the left-right symmetric shape become left-right asymmetric. It is convenient to illustrate such transformations using projections onto the 2D quadrupole-octupole space of variables α_{20} and α_{30}. The total energy is minimized over $\lambda = 4,\ldots,12$ and α_{22} deformation parameters and projected on $(\alpha_{20},\alpha_{30})$ plane as shown in Fig. 4.

As an illustration: For the $_{112}$Mo one finds that the Jacobi transition begins at spin L=50 $\hbar$ and terminates around L=74 $\hbar$. This shape evolution is followed by the Poincaré transition, whose upper spin limit is limited only by the vanishing of the fission barrier.

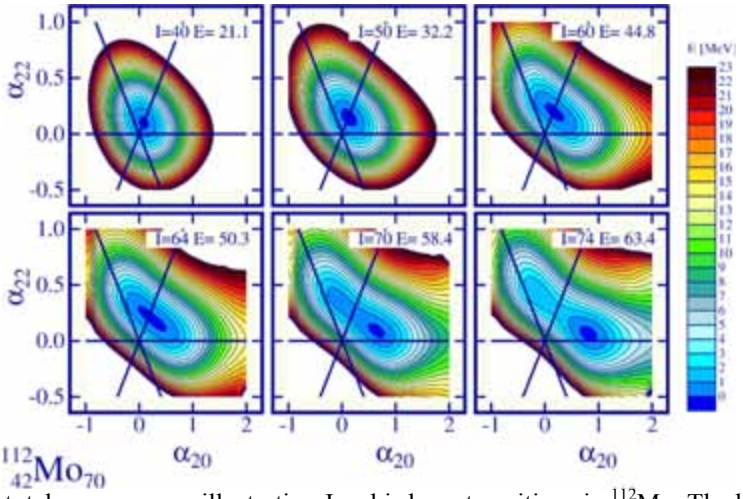

Figure 3: The total energy maps illustrating Jacobi shape transitions in ^{112}Mo. The horizontal line correspond to prolate shapes, whereas the straight lines with positive and negative inclinations correspond to oblate shapes. The minimum of energy (dark blue) is moving from oblate shapes (spin around L^{J}_{crit}=50 $\hbar$) to more and more elongated triaxial shapes (spins around 64-72 $\hbar$) to prolate deformation (above spin L=74 $\hbar$). In the boxes the yrast energy values are marked.

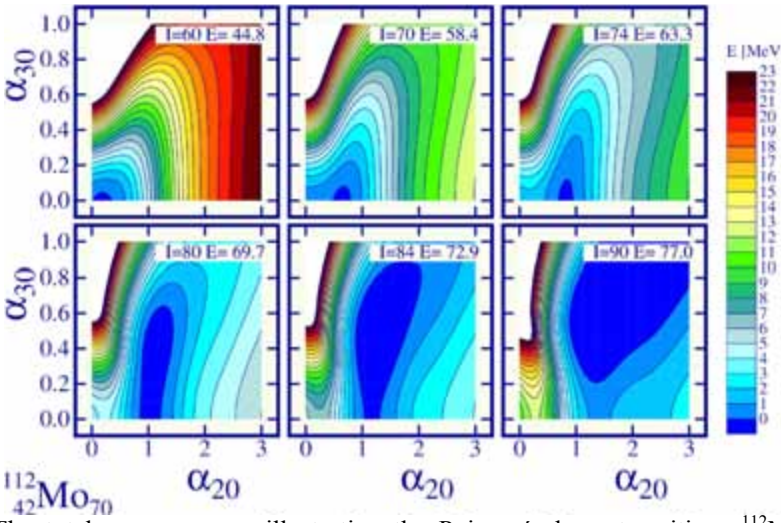

Figure 4: The total energy maps, illustrating the Poincaré shape transitions ^{112}Mo. Plot shows evolution of the minimum from octupole $\alpha_{30}=0$ L^{P}_{crit}=76 $\hbar$ up to $\alpha_{30}>0.6$ for spins above L=84 $\hbar$. In the boxes the yrast energy values are marked.

The nuclear deformation of the minimum of energy read out from maps (Fig. 3 and 4) are interpreted as the most probable static deformation for the given spin. Figure 5 presents the critical spin, for which the nucleus starts changing its shape from oblate to prolate by the non axial shapes – the Jacobi shape transition [12]. This starting point for the Jacobi transition for small fissility parameters is very weakly dependent on the congruence energy but it changes with the increasing the fissility of nuclei (red squares and blue dots). The end of Jacobi transition is manifesting in present calculations by the switching on the octupole deformation and other odd λ parameters ($\alpha_{30}>0.05$). The appearance of the octupole distortion of the fast rotating nucleus we would like to call: Poincaré shape transition [20, 21]. For heavy nuclei with huge fissility the nucleus does not persist spin high enough to observe the octupole deformation in the equilibrium shape. Other explanation can be the microscopic properties of heavy nuclei, which play the major role in the total energy. The very low spins of such nuclei still allow the existence of the shell and pairing effects. The potential energy maps (Fig. 3,4) suggest that in certain cases the energy changes very little whereas the deformation varies considerably around the absolute minimum. This leads to the large amplitude oscillation of the nuclear shape; such a motion can be conveniently described with the help of the collective Schrödinger equation:

$$\hat{H}_{\text{coll.}} = \frac{-h^2}{2\sqrt{B}} \sum_{i,j-1}^{n} \frac{\partial}{\partial \alpha^i} \left(\sqrt{B} B^{ij} \right) \frac{\partial}{\partial \alpha^j} + V \,. \tag{5}$$

Here, V is the collective nuclear potential calculated using the Liquid Drop Model, $B \equiv |\det[B_{ij}]$ is the absolute value of the determinant of the covariant

representation of the mass tensor. This expression is in fact the quantum version of the Hamiltonian with the classical kinetic energy as in:

$$T_{\text{class.}} = \frac{1}{2}\sum_{i,j} B_{ij}^{\text{class.}}(\alpha)\dot{\alpha}^i\,\dot{\alpha}^j. \tag{6}$$

where the symbols $\{\alpha^i\}$ represent the collective coordinates defining the equation of the nuclear surface. The inertia tensor must appear here in its covariant form in which case it is expressed in the units of MeV·s^2.

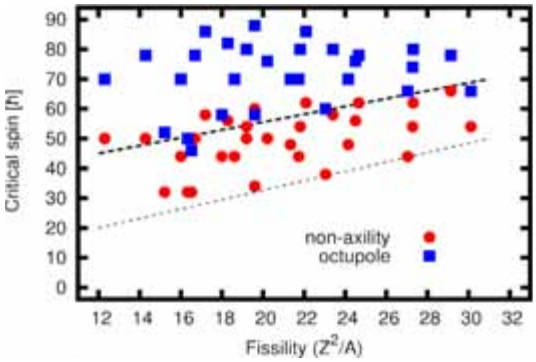

Figure 5: The critical spin for nuclei with mass A=40-200 when the nonaxiality start changing (beginning of Jacobi transition) and the spin when the octupole deformation is switched on ($\alpha_{30} > 0.05$ – beginning of the Poincaré transition). The dotted line gives the onset for Jacobi shape transition and dashed line roughly estimates the onset for Poincaré transitions. $\alpha_{30} > 0.05$

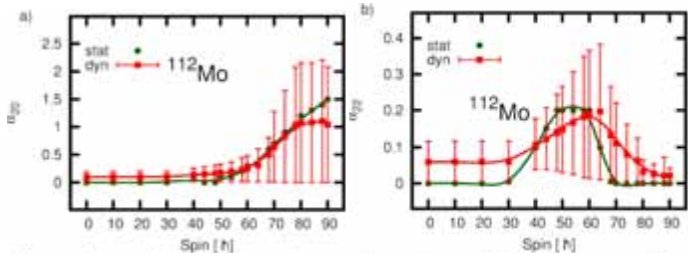

Figure 6: The dispersion of the dynamic quadrupole axial and non-axial deformation parameters displayed as a function of angular momentum and compared to static values for ^{112}Mo and constant inertia corresponding to $E_0 = 1$ MeV for L=0.

The tensor of inertia enters into the Hamiltonian in Eq. (5), and also through the 'reinterpretation' of the probability of finding the system in the curvilinear space. The latter probability is given by

$$d\,P_N(\alpha) = \Psi_N^*(\alpha)\Psi_N(\alpha)\sqrt{B(\alpha)}\,d\alpha\,, \tag{7}$$

where Ψ_N are the solutions of the collective Schrödinger equation

$$\hat{H}_{\rm coll.}\,\Psi_N = E_N\,\Psi_N \tag{8}$$

Here we do not calculate microscopically the inertia tensor and introduce the approximation by setting: $B_{\alpha_{22},\alpha_{22}} = B_{\alpha_{20},\alpha_{20}}$, and neglecting the non-diagonal term, $B_{\alpha_{22},\alpha_{20}} = B_{\alpha_{20},\alpha_{22}}$. Using the collective wave-functions, we calculate the most probable ('dynamic') quadrupole deformations, $(\alpha_{20},\alpha_{22})_{\rm dyn.}$. Our goal will be to compare the so obtained dynamic deformations to the static deformation, $(\alpha_{20},\alpha_{22})_{\rm stat.}$, the latter corresponding to the minimum on the potential energy surface. We may select as a measure of the most probable value of a given shape coordinate, $\alpha_{\lambda\mu}$, the associated r.m.s. values, $\bar{\alpha}_{\lambda\mu}$, defined by

$$\langle\alpha^2_{\lambda\mu}\rangle = \int {\rm d}\alpha \Psi^*_n(\alpha)\alpha^2_{\lambda\mu}\Psi_n(\alpha) \rightarrow \bar{\alpha}_{\lambda\mu} = \sqrt{\langle\alpha^2_{\lambda\mu}\rangle}. \tag{9}$$

The quantum character of the collective motion implies that each nuclear deformation should be associated with the probability density function $P(\alpha)$ so that the considered probabilities of finding the nucleus in a given 'shape interval', $[\alpha - {\rm d}\alpha, \alpha + {\rm d}\alpha]$ are given by

$${\rm d}P(\alpha) = 2\,|\Psi(\alpha)|^2 {\rm d}\alpha. \tag{10}$$

where $2\,d\alpha$ denotes the associated volume element in the deformation space. Consequently, a description of the nuclear motion in the shape space can be obtained through the expected values of the deformation, but also with the help of the spreading of the probability distribution described using the quadrupole dispersion coefficients:

$$\sigma_{20} \equiv \sqrt{\langle\alpha^2_{20}\rangle - \langle\alpha_{20}\rangle^2} \text{ and } \sigma_{22} \equiv \sqrt{\langle\alpha^2_{22}\rangle - \langle\alpha_{22}\rangle^2}. \tag{11}$$

The probability distribution is associated with the varying flatness of the energy landscapes in terms spin-dependent quantities: $\bar{\alpha}_{20}$ and σ_{20} as well as $\bar{\alpha}_{22}$ and σ_{22}. The quadrupole-octupole dispersion parameters are:

$$\sigma_{20} \equiv \sqrt{\langle\alpha^2_{20}\rangle - \langle\alpha_{20}\rangle^2} \text{ and } \sigma_{30} \equiv \sqrt{\langle\alpha^2_{30}\rangle - \langle\alpha_{30}\rangle^2}. \tag{12}$$

and estimated using Eq. (9). The potential energies in the case of the two-dimensional solutions using α_{20} and α_{30}, were obtained in such a way that at each $\{\alpha_{20},\alpha_{30}\}$, the minimization was performed over α_{22} as well as the axial symmetry deformations $\alpha_{\lambda 0}$ for $4 \le \lambda \le 12$. Figure 7 shows the influence of the collectivity on the range of spins with non-zero octupole deformations. The static prediction gives spin L=76 $\hbar$ as the beginning of the Poincaré transition.

When the zero point vibrations are taken into consideration, the dynamical deformation of the nucleus is changing within some range. This effect allows to expect lower critical spins for each transition than it was predicted in static case. The static limit for angular momentum is lowered almost by ten units. The discussion if Jacobi and Poincaré transitions are following each other or they could coexist in some range of spin is still open.

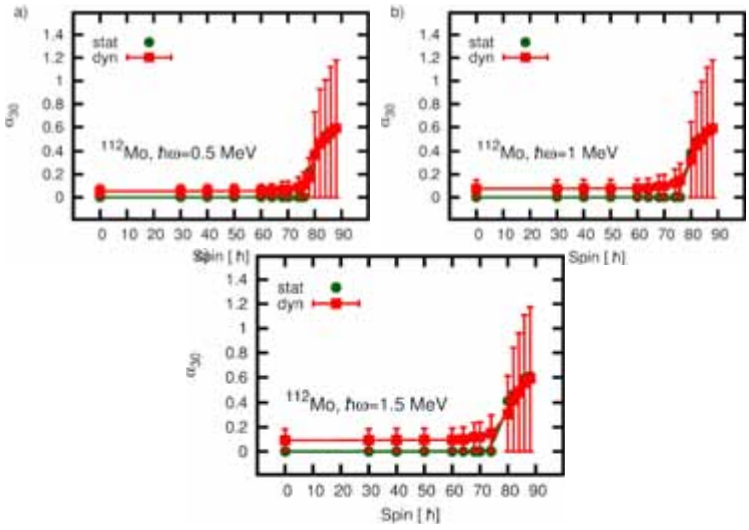

Figure 7: The dispersion of the dynamic octupole deformation displayed with the static deformation for the shapes on yrast line for ^{112}Mo. When the octupole deformation is switched on ($\alpha_{30} > 0.05$ – the Poincaré transition).

4. SUMMARY

The formula for the shape dependent congruence energy reproduces better the heights of the fission barriers. The fission barrier heights (Fig. 5) are reproduced significantly better for medium mass nuclei when the congruence energy is used.

The first estimates of the range of the nuclear fissility in which the Jacobi and Poincaré shape transitions are obtained with the help of the static deformations. These estimates provide rough experimental consitions for investigations of the Jacobi or Poincaré shape trasitions. The solution of the collective Schrödinger equation allows to take into account the large amplitude motion and to predict the dynamical deformations and their dispersion.

Similarly to ^{120}Cd described in Ref. [23], also for ^{112}Mo changing the average mass tensor does not influence the spin range for Poincaré transition but only the magnitude of the dispersion of the deformation parameter. The dynamic effects taken into account bring new and more realistic estimations of the variety of shapes expected for hot, rotating nuclei.

ACKNOWLEDGMENTS

This work has been supported by the COPIN-IN2P3 Polish-French Collaboration under Contract No. 05-119 and LEA COPIGAL project: “Search for the high-rank symmetries in subatomic physics“ and the Polish Ministry of Science and Higher

Education (Grant No. 2011/03/B/ST2/01894). We would like to thank A. Góźdź for discussions.

REFERENCES

1. Jacobi C.G.J., 1884. Vorlesungen über Dynamik; Ed. A. Clebsch, printed by G. Reimer, Berlin.
2. Poincaré H., 1885. Sur l'equilibre d'une masse fluide anime d'un mouvement de rotation, Acta Math. 7, 259.
3. Beringer R. and Knox W.J., 1961. Liquid-Drop Nuclear Model with High Angular Momentum, Phys. Rev. 121, 1195.
4. Möller P., Nix J.R., 1981. Nuclear mass formula with a Yukawa-plus-exponential macroscopic model and a folded-Yukawa single-particle potential , Nucl. Phys. A 361, 117; Atomic Masses and Nuclear Ground-State Deformations Calculated with a New Macroscopic Model, At. Data Nucl. Data Tables 39 (1988) 213.
5. Möller P., Madland D.G., Sierk A.J., Iwamoto A., 2001. Nuclear Fission Modes and Fragment Mass Asymmetries in a Five-Dimensional Deformation Space, Nature, London 409, 785.
6. Möller P., Sierk A.J., Bengtsson R., Sagawa H., Ichikawa T., 2009. Global Calculation of Nuclear Shape Isomers, Phys. Rev. Lett. 103, 212501.
7. Aberg S., Flocard H., Nazarewicz W., 1990. Nuclear Shapes in Mean Field Theory, Ann. Rep. Nucl. Part. Sci. 40, 439.
8. Egido J.L., Robledo L.M., Chasman R.R., 1997. Nuclear Shapes in 176W with Density Dependent Forces: From ground state to fission, Phys. Lett. B 393, 13.
9. Berger J.F., Girod M., Gogny D., 1989. Constrained hartree-fock and beyond, Nucl. Phys.A 502, 82c.
10. Pomorski K., Dudek J., 2003. Nuclear liquid-drop model and surface-curvature effects, Phys. Rev. C 67, 044316.
11. Dudek J., Pomorski K., Schunck N., Dubray N., 2004. Hyperdeformed and megadeformed nuclei: Lessons from the slow progress and emerging new strategies, Eur. Phys. J. A 20, 165.
12. Maj A. et al., 2004. Evidence for the Jacobi shape transition in hot 46Ti Nucl. Phys. A 731, 319.
13. Myers W.D., Swiatecki W.J., 1966. Nuclear Masses and Deformations Nucl. Phys. A 81, 1.
14. Kicinska-Habior M., Snover K.A, Behr J.A., Gossett C.A., Alhassid Y., Whelan N., 1993. Search for a Phase Transition in the Nuclear Shape at Finite Temperature and Rapid Rotation. Phys. Lett. B 308, 225.
15. Kmiecik M. et al., 2004. Probing nuclear shapes close to the fission limit with the giant dipole resonance in Rn216, Phys. Rev. C 70, 064317.
16. Maj A. et al., 2001. Search for Exotic Shapes of Hot Nuclei at Critical Angular Momenta, Nucl. Phys. A 687, 192.
17. Kmiecik M. et al., 2007. Strong Deformation Effects in Hot Rotating 46Ti, Acta Phys. Polon. B 38, 1437.
18. Kmiecik M. et al., 2005. GDR feeding of the highly-deformed band in 42Ca, Acta Phys. Polon. B 36, 1169.
19. CiemaŃa M. et al., 2011. Search for Jacobi Shape Transition in Hot Rotating 88Mo Nuclei Through Giant Dipole Resonance Decay. Acta Phys. Polon. B 42, 633.

20. Maj A., Mazurek K., Dudek J., Kmiecik M. and Rouvel D., 2010. Shape evolution at high spins and temperatures: nuclear Jacobi and Poincaré transitions, Int. J. Mod. Phys. E 19, 532.
21. Mazurek K., Dudek J., Kmiecik M., Maj A., Wieleczko J. P. and Rouvel D., 2011. Poincaré Shape Transitions in Hot Rotating Nuclei Acta Phys. Polon. B 42, 471.
22. Ivanyuk F. A. and Pomorski K., 2013. On the Poincaré instability of a rotating liquid drop Phys. Scr. T 154, 014021.
23. Mazurek K., Dudek J., Maj A., Rouvel D. 2015. Nuclear Jacobi and Poincaré transitions at high spins and temperatures: Account of dynamic effects and large-amplitude motion Phys. Rev. C 91, 034301.
24. Myers W. D., Swiatecki W. J., 1996. Nuclear Properties According to the Thomas-Fermi Model Nucl. Phys. A 601, 141.
25. Fan T. S., Jing K. X., Phair L., Tso K., McMahan M., Hanold K., Wozniak G. J., Moretto L. G., 2000. Excitation Functions and Mass Asymmetric Fission Barriers for Compound Nuclei 70, 76Se, Nucl. Phys. A 679, 121.
26. Delis D.N., et al, 1991. Mass Asymmetric Fission Barriers for 75Br, Nucl. Phys. A 534, 403.
27. Jing K.X., et al, 1999. Transition State Rates and Mass Asymmetric Fission Barriers of Compound Nuclei 90, 94, 98Mo, Nucl. Phys. A 645, 203.
28. Moretto L.G., Thompson S.G., Routti J., Gatti R.C., 1972. Influence of Shells and Pairing on the Fission Probabilities of Nuclei Below Radium, Phys. Lett. B 38, 471.